Statistical estimation of source location in presence of geoacoustic inversion uncertainty

Chen-Fen Huang
Institute of Oceanography, National Taiwan University, Taipei 10617, Taiwan
chenfen@ntu.edu.tw

Peter Gerstoft and William S. Hodgkiss
Marine Physical Laboratory, Scripps Institution of Oceanography, La Jolla, California 92093-0238
gerstoft@ucsd.edu, wsh@mpl.ucsd.edu

Abstract: A statistical estimation of source location incorporating uncertainty in ocean environmental model parameters is derived using a Bayesian approach. From a previous geoacoustic inversion, a posterior probability distribution of the environmental parameters that reflects uncertainty in the ocean environment is obtained. This geoacoustic uncertainty then is mapped into uncertainty in the acoustic pressure field and is propagated through the Bartlett matched-field processor for source localization. Using data from the ASIAEX 2001 East China Sea experiment, the estimated source location and variability over time are compared with the known source positions.

PACS numbers: 43.30.Pc, 43.30.Wi, 43.60.Pt [JL]
Date Received: December 22, 2008 **Date Accepted:** February 18, 2009

1. Introduction

This paper presents a statistical estimation of source location in the presence of ocean acoustic parameter environmental uncertainty. Many Bayesian approaches for increasing robustness to ocean environmental uncertainty have been developed.[1–7] Averaging over a uniform prior distribution of environmental parameters was proposed earlier in Refs. 1 and 2 as a method of improving robustness of source localization. Dosso and Wilmut[5,6] proposed a Bayesian focalization to quantify source localization with environmental uncertainty. In their Bayesian focalization approach all source positions and environmental parameters are inverted at once. For practical problems involving thousands of source positions, tracking is an efficient alternative. Kalman and particle filtering[4,7] can be used efficiently to track the source and geoacoustic parameters.

Estimation of uncertainty in environmental parameters for a single source-receiver range is well developed using Markov chain Monte Carlo (MCMC) Metropolis–Hasting sampling.[8–10] The processor derived in this paper translates the uncertainty in environmental parameters, which, for example, can be from a previous geoacoustic inversion, to the uncertainty in replica fields for matched-field source localization. The resulting processor is a weighted sum of Bartlett processors over the posterior probability distribution (PPD) of the environmental parameters. We demonstrate the approach using source tow data from the ASIAEX 2001 experiment.[8,11] Using the geoacoustic inversion results for source localization is well known;[12] the focus here is on the accompanying source position uncertainty.

2. Theory

Figure 1 summarizes the statistical estimation of source position using environmental information obtained from a previous geoacoustic inversion.

The classical matched-field processor consists of systematically placing a single frequency test point source at each point of a search grid, computing the acoustic field (replica) at all the elements of the array and then correlating this modeled field with the observed data from

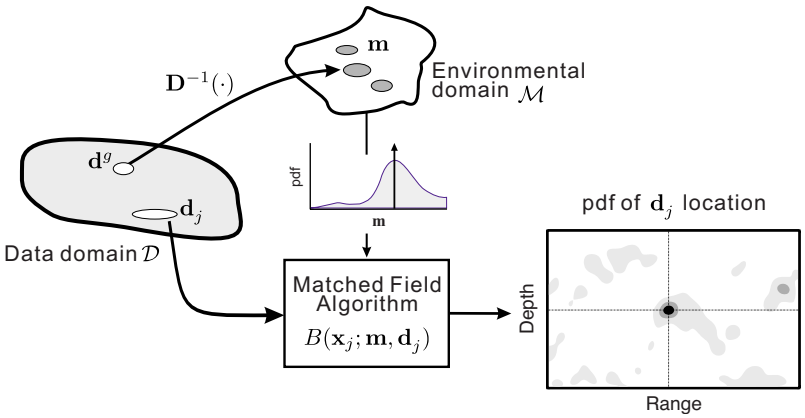

Fig. 1. (Color online) Measured data for source localization $\mathbf{d}_j$ ($\in\mathcal{D}$) is received at time j. From previous measured data $\mathbf{d}^g$ ($\in\mathcal{D}$) environmental parameters $\mathbf{m}$ ($\in\mathcal{M}$) are estimated via geoacoustic inversion along with a PPD of $\mathbf{m}$ that reflects its uncertainty. These environmental parameters then are mapped through a matched-field processor for statistically estimating the source location from $\mathbf{d}_j$.

an unknown source. In absence of data error and error in estimating the environmental parameter vector $\mathbf{m}$, the correlation is maximum when the test source location $\mathbf{x}$ is collocated with the true source

$$B(\mathbf{x}_j;\hat{\mathbf{m}},\mathbf{d}_j)=|\mathbf{w}(\mathbf{x}_j;\hat{\mathbf{m}})^H\mathbf{d}_j|^2=\mathbf{w}(\mathbf{x}_j;\hat{\mathbf{m}})^H\mathbf{R}_j\mathbf{w}(\mathbf{x}_j;\hat{\mathbf{m}}), \tag{1}$$

where $\mathbf{d}_j$ denotes the observed data at time index j, $\hat{\mathbf{m}}$ is an estimate of the parameter vector, and $\mathbf{w}(\mathbf{x};\hat{\mathbf{m}})=\mathbf{d}(\mathbf{x};\hat{\mathbf{m}})/|\mathbf{d}(\mathbf{x};\hat{\mathbf{m}})|$ is the normalized replica vector with the field solution $\mathbf{d}(\mathbf{x};\mathbf{m})$ computed from a acoustic model using the environmental parameter vector $\mathbf{m}$. When multiple snapshots are available, we assume that the signal source term can vary across snapshots, whereas the error power is the same for all snapshots. Then the observed data are efficiently expressed as a data covariance matrix $\mathbf{R}_j=\langle\mathbf{d}_j\mathbf{d}_j^H\rangle$.[13]

2.1 Posterior probability distribution of source position

The uncertainty in environmental parameters is translated to the uncertainty in replica fields for matched-field source localization.[8] The PPD of the source position at time j given the observation $\mathbf{d}_j$ is found via Bayes' rule

$$p(\mathbf{x}_j|\mathbf{d}_j)=\frac{p(\mathbf{d}_j|\mathbf{x}_j)p(\mathbf{x}_j)}{p(\mathbf{d}_j)}, \tag{2}$$

where $p(\mathbf{x}_j)$ is the probability density function (PDF) of $\mathbf{x}_j$ before observing the data. $p(\mathbf{d}_j|\mathbf{x}_j)$ is the likelihood function of the source position $\mathbf{x}_j$ at time step j given the data $\mathbf{d}_j$. This likelihood function can be derived from the PPD of $p(\mathbf{d}_j,\mathbf{m}|\mathbf{x}_j)$, by averaging over the environmental parameter vector $\mathbf{m}$ as follows:

$$p(\mathbf{d}_j|\mathbf{x}_j)=\int p(\mathbf{d}_j,\mathbf{m}|\mathbf{x}_j)\mathrm{d}\mathbf{m}=\int p(\mathbf{d}_j|\mathbf{m},\mathbf{x}_j)p(\mathbf{m}|\mathbf{x}_j)\mathrm{d}\mathbf{m}, \tag{3}$$

where $\mathbf{m}$ is independent of the source position $\mathbf{x}_j$ and the information about $\mathbf{m}$ was obtained from a previous geoacoustic inversion process using data $\mathbf{d}^g$. Therefore,

$$p(\mathbf{m}|\mathbf{x}_j)=p(\mathbf{m})=p(\mathbf{m}|\mathbf{d}^g). \tag{4}$$

The likelihood of the environmental parameters $\mathbf{m}$ and the source position $\mathbf{x}_j$ given $\mathbf{d}_j$ is determined from the assumption of data error statistics. The data error consists of both am-

bient noise as well as error in modeling the environment.[8] For simplicity, the error terms are assumed independent and identically distributed complex Gaussian random variables with variance ν as follows:

$$p(\mathbf{d}_j|\mathbf{m},\mathbf{x}_j,\nu)=\frac{1}{\pi^N\nu^N}\exp\left(-\frac{\phi(\mathbf{x}_j;\mathbf{m},\mathbf{d}_j)}{\nu}\right), \tag{5}$$

where $\phi(\mathbf{x}_j;\mathbf{m},\mathbf{d}_j)=\|\mathbf{d}_j\|^2-B(\mathbf{x}_j;\mathbf{m},\mathbf{d}_j)$ is the Bartlett objective function for the environmental parameter vector $\mathbf{m}$. Note that in Eq. (5) the complex source term has been estimated by a maximum likelihood approach[13] as opposed to integrating it out.[1] The uncertainty in the error variance ν is accounted for by integrating the complex Gaussian PDF over the nuisance parameter ν assuming a non-informative prior for ν (proportional to $1/\nu$) giving the likelihood function[11]

$$p(\mathbf{d}_j|\mathbf{m},\mathbf{x}_j)\propto\frac{1}{\phi(\mathbf{x}_j;\mathbf{m},\mathbf{d}_j)^N}, \tag{6}$$

where N is number of the hydrophones. Substituting Eqs. (6), (4), and (3) into Eq. (2) yields the PPD of $\mathbf{x}_j$ as

$$\begin{aligned}p(\mathbf{x}_j|\mathbf{d}_j)&=\frac{p(\mathbf{x}_j)}{p(\mathbf{d}_j)}\int p(\mathbf{d}_j|\mathbf{m},\mathbf{x}_j)p(\mathbf{m}|\mathbf{d}^g)\mathrm{d}\mathbf{m}\propto p(\mathbf{x}_j)\int\frac{1}{\phi(\mathbf{x}_j;\mathbf{m},\mathbf{d}_j)^N}p(\mathbf{m}|\mathbf{d}^g)\mathrm{d}\mathbf{m}\\&\propto p(\mathbf{x}_j)\sum_{k=1}^{K}\frac{1}{\phi(\mathbf{x}_j;\mathbf{m}_k,\mathbf{d}_j)^N},\end{aligned} \tag{7}$$

where $\phi(\mathbf{x}_j;\mathbf{m}_k,\mathbf{d}_j)$ is the Bartlett objective function for an environmental parameter vector $\mathbf{m}_k$ sampled by a MCMC algorithm. The statistical estimation of source position is based on Eq. (7).

3. Results

Data on a vertical line array from the ASIAEX 2001 East China Sea experiment in 106.5-m water depth are used to illustrate the approach.[8] First, an inversion was carried out at source-receiver range of 1.7 km, indicated by a circle in Fig. 2(a). An environment with 13 unknown parameters with their search bounds indicated in Fig. 2(b) was estimated, including geometrical, geoacoustic, and ocean sound speed empirical orthogonal function coefficients.[8] The inversion was based on a MCMC sampling giving samples $\mathbf{m}_k$ from which the PPD $p(\mathbf{m}|\mathbf{d}^g)$ could be estimated and subsequently used as prior information for source localization with new data $\mathbf{d}_j$. Based on Eq. (7), the samples $\mathbf{m}_k$ corresponding to a particular environment then are combined with the source position data $\mathbf{d}_j$ via the objective function $\phi(\mathbf{x}_j;\mathbf{m}_k,\mathbf{d}_j)$ for each possible location $\mathbf{x}_j$. The prior distribution $p(\mathbf{x}_j)$ was assumed uniform with the depth-range search interval. Summing over all samples gives the PPD of source location $p(\mathbf{x}_j|\mathbf{d}_j)$.

To estimate statistically the source position given the environmental information obtained from the inversion, a measured data vector $\mathbf{d}_j$ is used where the source range was 2.5 km. The source signal was a cw tone at 195 Hz. The signal-to-noise ratio (SNR) was estimated to be 16.3 dB using the ratio of the mean power received in the signal frequency fast Fourier transform bin and the (assumed to be noise) power received outside this bin. The observed data cross spectral density matrix $\mathbf{R}$ is normalized by the largest eigenvalue of the matrix, so that the maximum signal power is 1. For simulation purposes, the desired SNR is generated by varying the noise variance ν_n according to the array SNR definition[8]

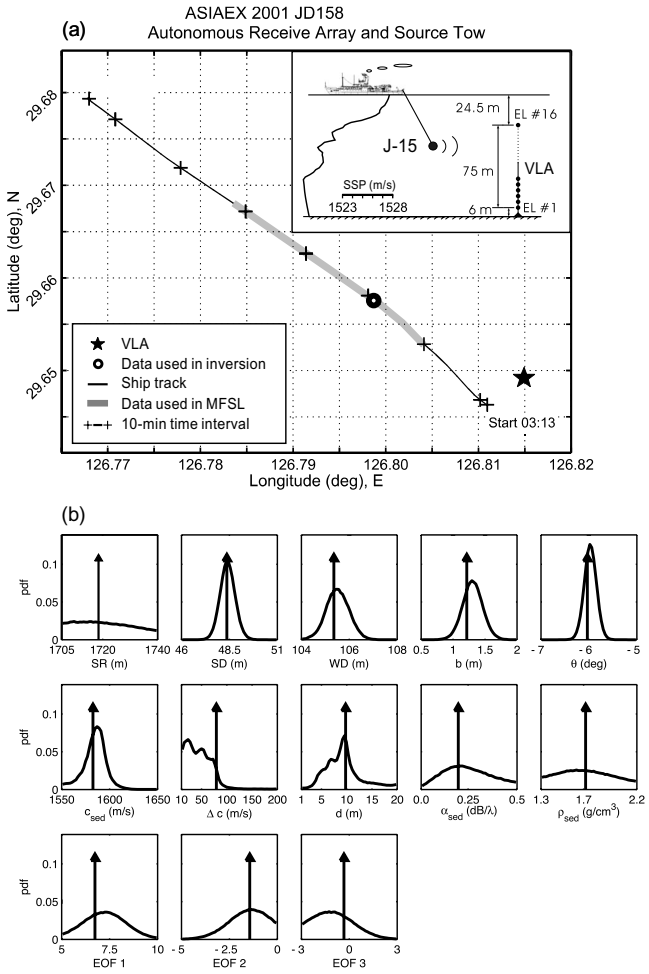

Fig. 2. (a) Track of R/V *Melville* during the ASIAEX 2001 East China Sea experiment. The experimental geometry is shown in the upper right-hand corner of the figure. (b) 1D marginal posterior probability densities and MAP (indicated by arrows) of the model parameters using the measured data obtained at approximately 1.7 km from the source.

$$\mathrm{SNR} = 10 \log \frac{1}{\nu_n} \quad \text{where } \nu_n = \frac{E[\|\mathbf{n}\|^2]}{N} \tag{8}$$

and $\mathbf{n}$ is the noise in the data (the array SNR should not be confused with the element SNR used in, e.g., Ref. 5). Since noise only can be added to the data, we only can lower the SNR from the maximum of 16.3 dB.

The parameter uncertainties are mapped through to the statistical estimation of source localization using Eq. (7). The replica vector for a hypothesized source position $\mathbf{x}$ and for each environmental parameter vector $\mathbf{m}_k$, $\mathbf{w}(\mathbf{x};\mathbf{m}_k)$, is computed using the normal mode propagation model SNAP.[14] Monte Carlo subsampling[8] of the geoacoustic inversion samples is used to evaluate Eq. (7) with $K=900$. The range-depth search grid spacing is 8 m in range from 1500 to 3500 m and 1.4 m in depth from 1 to 99 m.

Figure 3(a) shows the effect of the array SNR on the PPD of source range and depth at a source frequency of 195 Hz and range 2.5 km. The intersection of the lines indicates the peak of the PPD, and the darkest region indicates the 50% highest posterior density (HPD) in which

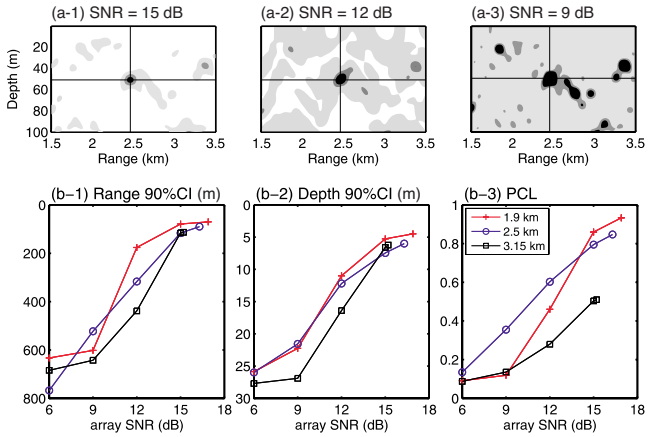

Fig. 3. (Color online) (a) Realizations of PPD of source range and depth for 195 Hz at 2.5 km range for three SNRs. Each panel shows the MAP source position (intersection of thin lines) and the HPD of source position [with 50% (dark), and 75% and 99% (light)]. (b) Source position uncertainty versus SNR for ranges 1.9 (+), 2.5 (○), and 3.15 km (□): (1) and (2) 90% CI, and (3) PCL in a region around the assumed source position.

the source falls given the observed data $\mathbf{d}_j$ and the environmental uncertainty. The range-depth PPD for the various SNRs [Figs. 3(a)(1)–3(a)(3)] shows that the number of competing peaks increases as SNR decreases. Note that the range-depth PPD for low SNR depends on the noise realization. The benefit here is not only we have the maximum *a posteriori* (MAP) estimate of source position but also the level of uncertainty.

The effect of SNR on the source position uncertainties is displayed for three source ranges in Fig. 3(b). The estimated SNRs in the observed data for ranges of 1.9, 2.5, and 3.15 km are 16.9, 16.3, and 15.2 dB, respectively (estimated using adjacent bins, see above). In Figs. 3(b)(1) and 3(b)(2) the 90% credibility interval (CI) extracted from the one-dimensional (1D) marginal distribution is shown. At lower SNR, the noise dominates the uncertainty of source position. For high SNR, the source position uncertainty will not approach zero since uncertainty in the environmental parameters will dominate. From the PPD surfaces in Fig. 3(a) we can

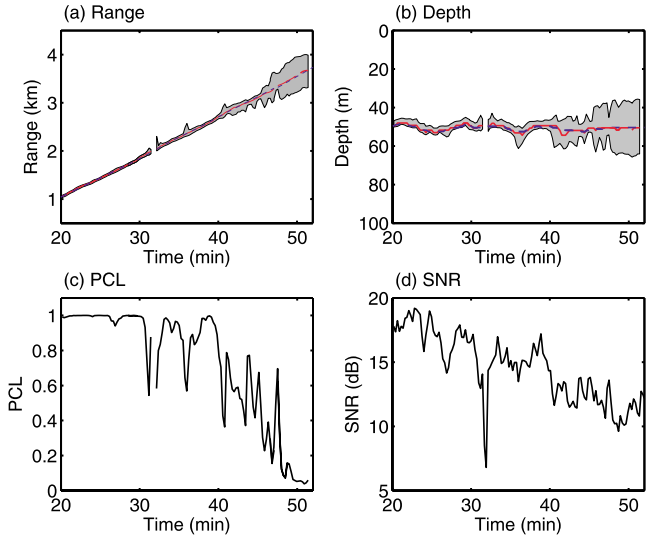

Fig. 4. (Color online) MAP estimate of source range (a) and depth (b) (solid) and their 90% CI (gray area) from time 20 to 52 min. The dashed line indicates the range measured by differential global positioning system (a) and the depth by a depth sensor (b). (c) PCL and (d) SNR estimated from the data.

integrate a region around the source position (an acceptable region of 20 m in depth and 200 m in range) obtaining the probability of correct localization (PCL) (Ref. 2) (this also has been termed integrated probability).[5] The PCL increases with SNR and tends to decrease with range.

As part of the experiment, a source tow from 1 to 3.7 km was performed. Using the estimated geoacoustic parameters and their uncertainty as well as the methodology above the MAP estimate of source position and the 90% CI is presented in Figs. 4(a) and 4(b). Furthermore, Figs. 4(c) and 4(d) show that as the SNR decreases so does the PCL.

4. Summary

Source position estimation in the presence of ocean environment uncertainty is investigated using the ASIAEX 2001 source tow data. A simulation shows that the noise deteriorates the localization performance at lower SNR, while the uncertainty in the ocean environment dominates at higher SNR. Continuous localization using the source tow data indicates that the localization uncertainty increases with range and 1/SNR.

Acknowledgments

This work was supported by the following: contract NSC96-2218-E-019-003 from the National Science Council of Taiwan; contract 96C100303 from the Ministry of Education of Taiwan under the project entitled Aim for Top University–Asian Pacific Ocean Research Center (to C.-F.H.); and Grant No. N00014-05-1-0264 from the Office of Naval Research.

References and links

[1]A. M. Richardson and L. W. Nolte, "*A posteriori* probability source localization in an uncertain sound speed, deep ocean environment," J. Acoust. Soc. Am. **89**, 2280–2284 (1991).
[2]J. A. Shorey, L. W. Nolte, and J. L. Krolik, "Computationally efficient Monte Carlo estimation algorithms for matched field processing in uncertain ocean environments," J. Comput. Acoust. **2**, 285–314 (1994).
[3]J. A. Shorey and L. W. Nolte, "Wideband optimal *a posteriori* probability source localization in an uncertain shallow ocean environment," J. Acoust. Soc. Am. **103**, 355–361 (1998).
[4]S. L. Tantum and L. W. Nolte, "Tracking and localizing a moving source in an uncertain shallow water environment," J. Acoust. Soc. Am. **103**, 362–373 (1998).
[5]S. E. Dosso and M. J. Wilmut, "Bayesian focalization: Quantifying source localization with environmental uncertainty," J. Acoust. Soc. Am. **121**, 2567–2574 (2007).
[6]S. E. Dosso and M. J. Wilmut, "Uncertainty estimation in simultaneous Bayesian tracking and environmental inversion," J. Acoust. Soc. Am. **124**, 82–97 (2008).
[7]C. Yardim, P. Gerstoft, and W. S. Hodgkiss, "Tracking of geoacoustic parameters using Kalman and particle filters," J. Acoust. Soc. Am. **125**, 746–760 (2009).
[8]C.-F. Huang, P. Gerstoft, and W. S. Hodgkiss, "Validation of statistical estimation of transmission loss in the presence of geoacoustic inversion uncertainty," J. Acoust. Soc. Am. **120**, 1932–1941 (2006).
[9]Y.-M. Jiang, N. R. Chapman, and M. Badiey, "Quantifying the uncertainty of geoacoustic parameter estimates for the New Jersey shelf by inverting air gun data," J. Acoust. Soc. Am. **121**, 1879–1894 (2007).
[10]J. Dettmer, S. E. Dosso, and C. W. Holland, "Model selection and Bayesian inference for high-resolution seabed reflection inversion," J. Acoust. Soc. Am. **125**, 706–716 (2009).
[11]C.-F. Huang, P. Gerstoft, and W. S. Hodgkiss, "Uncertainty analysis in matched-field geoacoustic inversions," J. Acoust. Soc. Am. **119**, 197–207 (2006).
[12]D. F. Gingras and P. Gerstoft, "Inversion for geometric and geoacoustic parameters in shallow water: Experimental results," J. Acoust. Soc. Am. **97**, 3589–3598 (1995).
[13]P. Gerstoft and C. F. Mecklenbräuker, "Ocean acoustic inversion with estimation of *a posteriori* probability distributions," J. Acoust. Soc. Am. **104**, 808–819 (1998).
[14]F. B. Jensen and M. C. Ferla, *SNAP: The SACLANTCEN Normal-Mode Acoustic Propagation Model* (SACLANT Undersea Research Centre, SM 121, La Spezia, Italy, 1979).